Journal of Peptide Science
J. Peptide Sci. **9**: 64–74 (2003)
Published online in Wiley InterScience (www.interscience.wiley.com). DOI: 10.1002/psc.433

JOURNAL OF
PEPTIDE SCIENCE

Conformational Investigation of α, β-Dehydropeptides. XI. Molecular and Crystal Structure of Ac-(*Z*)-ΔPhe-NMe$_2$ as Compared to those of Related Molecules†

DAWID SIODŁAK,[a] MAŁGORZATA A. BRODA,[a] BARBARA RZESZOTARSKA,[a]* IZABELA DYBAŁA[b] and ANNA E. KOZIOŁ[b]

[a] Institute of Chemistry, University of Opole, 45-052 Opole, Poland
[b] Faculty of Chemistry, Maria Curie-Skłodowska University, 20-031 Lublin, Poland

Received 19 May 2002
Revised 18 July 2002

Abstract: A series of three homologous dimethyldiamides Ac-(*Z*)-ΔPhe-NMe$_2$, Ac-L-Phe-NMe$_2$ and Ac-DL-Phe-NMe$_2$ have been synthesized and their structures determined from single-crystal X-ray diffraction data. To learn more about the conformational preferences of the compounds studied, the fully relaxed ϕ, ψ conformational energy maps on the free molecules of Ac-ΔAla-NMe$_2$ and Ac-(*Z*)-ΔPhe-NMe$_2$ were obtained with the HF/3-21G method and the calculated minima re-optimized with the DFT/B3LYP/6-31G** method. The crystal state results have been compared with the literature data. The studied dimethyldiamide Ac-ΔXaa-NMe$_2$ combines the double bond in positions α, β and the *C*-terminal tertiary amide within one molecule. As the representative probe with ΔXaa = ΔAla, (*Z*)-ΔLeu and (*Z*)-ΔPhe shows, in the solid state they adopt the conservative conformation with ϕ, $\psi \sim -45^\circ$, $\sim 130^\circ$ and with a non-planar tertiary amide bond, whatever the packing forces are. This conformation is located on the Ramachandran map in region H/F, which is of high-energy for common amino acids, but not so readily accessible to them. The free molecule calculations on Ac-ΔAla-NMe$_2$ and Ac-(*Z*)-ΔPhe-NMe$_2$ reveal that, in spite of dissimilar overall conformational profiles of these molecules, this structure is one of their low-energy conformers and for Ac-(*Z*)-ΔPhe-NMe$_2$ it constitutes the global minimum. So, the theoretical results corroborate those experimental results proving that this structure is robust enough to avoid conformational distortion due to packing forces. In contrast to Ac-ΔXaa-NMe$_2$, the saturated Ac-L/DL-Xaa-NMe$_2$ shows the constancy of the associative patterns but do not prefer any molecular structure in the solid state.

Keywords: dimethylamides; X-ray crystallography; phenylalanine derivatives; α, β-dehydro amino acids; amino acid amides; dehydropeptides; (*Z*)-dehydrophenylalanine derivative; *ab initio* calculations

INTRODUCTION

An essential point in the strategy for peptide-targeted molecular design is the introduction of a specialized amino acid into the elaborated molecule, which confers local constraints on the backbone main chain and the side chain moiety [3–5]. A type of specialized amino acids, found in both nature and used by researchers, are the α, β-dehydro amino acids. Their unique α, β-double bond with the β-substituent(s) provides some steric conformational

Abbreviations: Δ, α, β-dehydro; Tle, pseudoleucine.

* Correspondence to: Barbara Rzeszotarska, Institute of Chemistry, University of Opole, Oleska Str. 48, 45-052 Opole, Poland; e-mail: rzeszot@uni.opole.pl
† For Part X in this series see Ref [1]. Presented in part at the 16th Polish Peptide Symposium, Kraków, September 2001 [2].
Contract/grant sponsor: University of Opole; Contract/grant number: 9/ICh/2002-W.
Contract/grant sponsor: Academic Computer Center CYFRONET AGH of Kraków; Contract/grant number: KBN/SGI2800/UOpolski/011/2001.

constraint to the peptide backbone torsion ϕ, ψ angles and also restriction of the orientation of the amino acid side chain. This decreases considerably the flexibility of linear peptides and fixes the side chain χ^1 angle either to the (*Z*) or (*E*) position. Of the unsaturated amino acids, the most commonly used modifier is (*Z*)-dehydrophenylalanine. On the other hand, many modifications of peptides and peptidomimetics are based on the tertiary amide bond. The *C*-terminus of some bioactive peptides can be synthetically processed to *N*′, *N*′-dimethylamide [6]. The tertiary amides constitute a unit of *N*-methyl peptides that have been known for a long time [7–13] and are the basic unit of peptoid peptidomimetics, a relatively new class of potential pharmacological tools and drugs [14]. For simplicity of structural investigation, the tertiary amide can be modelled by the *N*′, *N*′-dimethylamide group.

We synthesized Ac-(*Z*)-ΔPhe-NMe$_2$, which combines the (*Z*)-dehydrophenylalanine residue and the *N*′, *N*′-dimethylamide grouping within one molecule, and studied its conformational properties in the solid state by X-ray diffraction and in the gas phase by HF and DFT calculations. For structural comparisons, Ac-L-Phe-NMe$_2$ and Ac-DL-Phe-NMe$_2$ have been synthesized and their crystal structures solved and free molecule calculations performed on Ac-ΔAla-NMe$_2$ of known crystal structure [1].

MATERIALS AND METHODS

General Synthetic Procedures

Ac-DL-Phe was obtained according to [15] and Ac-(*Z*)-Δ-Phe according to [16]. The reaction progress was monitored and the homogeneity of the products roughly checked on silica gel plates (TLC aluminium sheets, silica gel 60; Merck 105553) in the solvent systems (v/v): $CHCl_3$/dioxane/MeOH/NH_4OH concd. (12 : 5 : 4 : 1); $CHCl_3$/Py/AcOH (21 : 2 : 1); $CHCl_3$/Py/AcOH (120 : 6 : 5); $CHCl_3$/MeOH/ AcOH (190 : 15 : 6); $CHCl_3$/MeOH (5 : 1). Spots were visualized with chlorine-tolidine reagent for saturated compounds and with fluorescein-bromine for dehydrophenylalanine derivatives. The solvents from the reaction mixtures and from the fractions after column chromatography were removed *in vacuo* on a rotary evaporator at a bath temperature not exceeding 30 °C. Melting points were determined using a DSC-2010 calorimeter (Thermal Analysis Instruments) under nitrogen in a closed copper vessel with a heating rate of 10 °C·min^{-1}. HPLC was performed on a Beckman 'System Gold' chromatograph consisting of a Model 126 programmable module, a Model 168 diode array detector (working at 210 nm) and a Model 210A injection. An Alltech Alltima, C_{18}, 5 µm, 150 × 4.6 mm reversed-phase column and 0.1% TFA/acetonitrile (80 : 20) as a mobile phase were used. ^{1}H NMR spectra were recorded on a spectrometer Tesla BS 567 (100 MHz) in $CDCl_3$ with internal tetramethylsilane standard.

Ac-(Z)-ΔPhe-NMe$_2$

Isobutyl chlorocarbonate (0.65 ml, 5 mmol) was added dropwise to a stirred and cooled (−15 °C) solution of Ac-(*Z*)-ΔPhe (1.03 g, 5 mmol) and *N*-methylmorpholine (0.55 ml, 5 mmol) in dimethyl formamide (8 ml) and tetrahydrofuran (2 ml). After 15 min, this was followed by a 5 M solution of dimethylamine (15 mmol) in tetrahydrofuran (3.0 ml). Stirring was continued at −15 °C for 1 h and at 20 °C overnight. The solvents were evaporated. The residue was dissolved in ethyl acetate (50 ml) and extracted with saturated $NaHCO_3$ (10 ml), 5% HCl (3 × 10 ml) and brine (3 × 10 ml). Ethyl acetate was evaporated and the residue crystallized from ethyl acetate/*n*-hexane. Yield: 0.72 g (62%). Mp 154.89 °C; HPLC: $t_R = 10.23$ min, 99.2% purity. NMR δ: 2.1 (s, 3H, Ac), 3.0, 3.1 (2s, 6H, NMe$_2$), 5.7 (s, 1H, C$^\beta$ H), 7.4 (m, 5H, Ph), 9.0 (s, 1H, NH). Analysis for $C_{13}H_{16}N_2O_2$ Calcd. C 67.21, H 6.94, N 12.06 Found C 67.18, H 6.89, N 12.11.

Ac-L-Phe-NMe$_2$

Isobutyl chlorocarbonate (0.65 ml, 5 mmol) was added dropwise to a stirred and cooled (−15 °C) solution of Z-Phe (1.50 g, 5 mmol) and *N*-methylmorpholine (1.10 ml, 10 mmol) in tetrahydrofuran (7 ml). After 15 min, this was followed by a 5 M solution of dimethylamine (15 mmol) in tetrahydrofuran (3 ml). Stirring was continued at −15 °C for 2 h and then at 7 °C for 2 h. The solvent was evaporated, the residue dissolved in ethyl acetate (20 ml) and extracted with water (2 × 5 ml), saturated $NaHCO_3$ (5× 5 ml), water (2 × 5 ml), 10% HCl (5 ml) and water (2 × 5 ml). Ethyl acetate was evaporated and the residue dissolved in methanol (10 ml). Water (2 ml) and Pd/C (300 mg) were added, hydrogen was bubbled for 60 min and the catalyst was filtered off. The solvents were evaporated and the residue was dissolved in chloroform (15 ml), cooled to −15 °C and triethylamine (0.7 ml, 5 mmol) and acetyl chloride (0.35 ml, 5 mmol) were added dropwise under stirring. Stirring was continued at −15 °C for 1 h and chloroform evaporated. The white powder was dissolved in water (15 ml), applied to a Dowex 2 × 8 column in OH^- form (11.5 mmol) and eluted with water. Appropriate evaporated fractions (0.85 g) were dissolved in ethyl acetate (5 ml) and *n*-hexane (2 ml) was added. The resulting precipitate was filtered off and discarded. Ethyl acetate (1 ml) was added to the filtrate and the product was precipitated with *n*-hexane. Yield: 0.55 g (47%). Mp 118.74 °C; $[\alpha]_D^{24.3} = 55.04 \pm 0.04°$(c 1, water) (a polarimeter Jasco DIP-1000); HPLC: $t_R = 10.8$ min, 99.6% purity. NMR δ: 2.0 (s, 3H, Ac), 2.7, 2.9 (2s, 6H, NMe_2), 3.0 (d, 2H, CH_2), 5.2 (m, 1H, $C^\alpha H$), 6.9 (s, 1H, NH), 7.1 (m, 5H, Ph). Analysis for $C_{13}H_{18}N_2O_2$ Calcd. C 66.64, H 7.74, N 11.96 Found C 66.52, H 7.84, N 12.08.

Ac-DL-Phe-NMe$_2$

Isobutyl chlorocarbonate (1.3 ml, 10 mmol) was added dropwise to a stirred and cooled (−15 °C) solution of Ac-DL-Phe (2.07 g, 10 mmol) and *N*-methylmorpholine (1.1 ml, 10 mmol) in tetrahydrofuran (10 ml). After 15 min, this was followed by a 5 M solution of dimethylamine (30 mmol) in tetrahydrofuran (6 ml). Stirring was continued at −15 °C for 2 h and at −5 °C for 2 h, the solvent was evaporated, the residue dissolved in water (10 ml), applied to a Dowex 2 × 8 column in OH^- form (20 mmol) and eluted with water. The appropriate evaporated fractions were crystallized from ethyl acetate (10 ml)/*n*-hexane. Yield: 1.14 g (49%). Mp. 100.55 °C (lit. [17] mp 99°–100 °C); HPLC: $t_R = 10.8$ min, 100.0% purity. NMR: as for L-compound. Analysis for $C_{13}H_{18}N_2O_2$ Calcd. C 66.64, H 7.74, N 11.96 Found C 66.73, H 7.51, N 11.67.

X-Ray Crystal Analysis

Data collection for single crystals was carried out at room temperature on a four circle KM4 diffractometer using CuKα radiation (λ = 1.54178 Å). Reflections were collected up to $\theta_{max} = 80°$, and corrected for Lorentz and polarization effects. Crystal structures were solved by direct methods [18] and refined by full-matrix least-squares on F^2 using the program SHELXL-97 [19]. H-atoms were positioned initially on difference maps, and a 'riding model' was applied during the refinement. The non-hydrogen atoms were refined with anisotropic displacement parameters. The crystallographic data and structure refinements for three sample compounds are collected in Table 1. Further details of the crystal structures reported in this paper have been deposited at the Cambridge Crystallographic Data Centre. Copies of

Table 1 Crystallographic Data and Structure Refinement Parameters for Ac-(*Z*)-ΔPhe-NMe$_2$, Ac-L-Phe-NMe$_2$ and Ac-DL-Phe-NMe$_2$

	Ac-(*Z*)-ΔPhe-NMe$_2$	Ac-L-Phe-NMe$_2$	Ac-DL-Phe-NMe$_2$
Crystal system	Triclinic	Orthorhombic	Triclinic
Space group	$P\bar{1}$	$P2_12_12_1$	$P\bar{1}$
Z	2	4	2
Cell dimensions			
a (Å)	8.354(2)	9.356(2)	7.589(2)
b (Å)	9.144(2)	9.441(2)	9.622(2)
c (Å)	9.423(1)	15.128(3)	10.643(2)
α (°)	67.11(3)		65.83(3)
β (°)	81.94(3)		70.64(3)
γ (°)	74.81(3)		70.00(3)
Calculated density (g·cm^{-3})	1.207	1.165	1.198
Volume (Å^3)	639.4(2)	1336.3(5)	649.4(2)
Number of independent reflections [R(int)]	2232 [0.090]	1636	2701 [0.076]
Absorption coefficient [Cu Kα] (mm^{-1})	0.667	0.639	0.657
Extinction coefficient	0.019(3)	0.018(3)	0.17(2)
Final *R* indices [$I > 2\sigma(I)$]	$R1 = 0.0750$	$R1 = 0.0571$	$R1 = 0.0708$
	$wR2 = 0.1529$	$wR2 = 0.1571$	$wR2 = 0.1905$
Residual electron density max; min (e Å^{-3})	0.29; −0.18	0.21; −0.19	0.31; −0.24

the data can be obtained free of charge on application to the Director, CCDC, 12 Union Road, Cambridge CB2 1EZ, UK (fax: +44-(0) 1223-336033 or e-mail: deposit@chemcryst.cam.ac.uk) and on quoting the full journal citation.

Computational Procedures

Fully relaxed (ϕ, ψ) conformational energy maps for the free Ac-ΔAla-NMe$_2$ and Ac-(*Z*)-ΔPhe-NMe$_2$ molecules were performed with the HF/3-21G method on a grid of points with 15° and 30° spacing, respectively. The HF optimized conformers served as starting structures for full re-optimization of all degrees of freedom at the DFT level with the B3LYP hybrid functional [20] and the 6-31G** basis set. All calculations were carried out using the Gaussian 98 package [21]. Their detailed results can be obtained on request from the corresponding author.

RESULTS

Molecular and Crystal Structure

The bond lengths and angles of the three sample compounds, involving the sp^2 C$^\alpha$/C$^\beta$ atoms, are as expected for common amino acid derivatives [22] including Ac-Xaa-NMe$_2$ [1]. For the ΔPhe moiety, they agree with the average bond lengths and angles given for this residue [23]. Figure 1 depicts the stereo views and Table 2 lists the values of torsion angles of these molecules. The torsion angles ϕ, ψ defining the peptide main chain and the torsion angle χ^2 defining the orientation of the phenyl plane were ϕ, ψ, $\chi^2 = -49.5°$, 132.6°, −26.4° for Ac-(*Z*)-ΔPhe-NMe$_2$; ϕ, ψ, $\chi^2 = -99.3°$, 148.5°, 94.1° for L-compound, and ϕ, ψ, $\chi^2 = -80.7°$, 156.8°, 107.9° for the DL-species. All secondary amides are *trans* and the orientation of two carbonyl groups within each molecule is *cisoid*. Figure 2 shows the fit of all three molecules through the C1-C2-N2 fragment. As seen, the *C*-termini, with its main feature the dimethylamide, essentially assumes a similar conformation. Angles ψ differ by not more than 24°. However, the conformation of the *N*-termini and phenyl ring position can vary significantly. While the differences in angles ϕ, and χ^2 between the L and DL structures do not exceed 20°, these angles are strongly affected by the α,β-double bond and the difference between the L/DL- and Δ-compound reaches ~50° for angle ϕ and up to ~130° for angle χ^2. The dimethylamide group out-of-plane

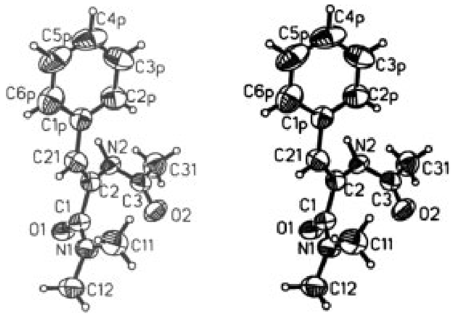

Ac-(Z)-ΔPhe-NMe$_2$

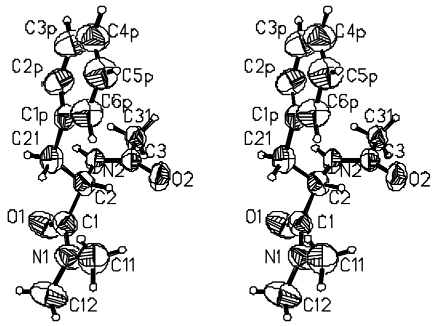

Ac-L-Phe-NMe$_2$

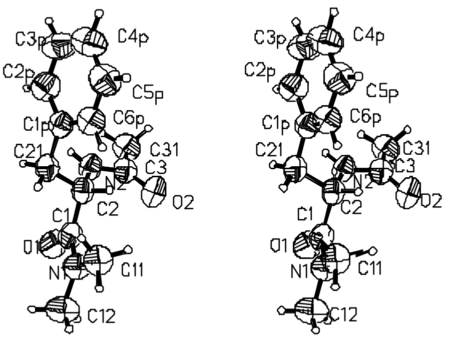

Ac-DL-Phe-NMe$_2$

Figure 1 Stereo drawing of the X-ray diffraction structure of Ac-(Z)-ΔPhe-NMe$_2$, Ac-L-Phe-NMe$_2$ and Ac-DL-Phe-NMe$_2$.

parameters [14,24,25] indicate a higher degree of non-planarity within the Δ-molecule than within the L/DL-species.

Figure 3 depicts the characteristic fragments of crystal packing in the investigated compounds. The main driving force for their association is the NH...O=C hydrogen bonding. Both Ac-ΔPhe-NMe$_2$ and Ac-DL-Phe-NMe$_2$ molecules form centrosymmetric dimers with the N2H...O1=C hydrogen bonds. Ac-L-Phe-NMe$_2$ molecules bind in infinite chains by

Table 2 Selected Geometric Parameters for Ac-(*Z*)-ΔPhe-NMe$_2$, Ac-L-Phe-NMe$_2$ and Ac-DL-Phe-NMe$_2$

		Ac-(*Z*)-ΔPhe-NMe$_2$	Ac-L-Phe-NMe$_2$	Ac-DL-Phe-NMe$_2$
Torsion angles (°)				
Φ	C(3)-N(2)-C(2)-C(1)	−49.5(6)	−99.3(6)	−80.7(4)
Ψ^1	N(1)-C(1)-C(2)-N(2)	132.6(5)	148.5(5)	156.8(3)
Ψ^2	O(1)-C(1)-C(2)-N(2)	−50.6(7)	−34.9(8)	−26.1(4)
Ψ^3	O(1)-C(1)-C(2)-C(21)	119.0(6)	86.0(7)	95.4(4)
Ψ^4	N(1)-C(1)-C(2)-C(21)	−57.9(7)	−90.6(6)	−81.7(4)
ω_1	C(2)-N(2)-C(3)-C(31)	173.0(4)	177.9(5)	178.7(3)
$\omega_2{}^1$	C(12)-N(1)-C(1)-C(2)	173.0(4)	176.3(7)	176.1(3)
$\omega_2{}^2$	O(1)-C(1)-N(1)-C(11)	168.3(5)	−176.6(7)	179.0(3)
$\omega_2{}^3$	O(1)-C(1)-N(1)-C(12)	−3.8(7)	−0.2(10)	−1.1(5)
$\omega_2{}^4$	C(11)-N(1)-C(1)-C(2)	−14.9(7)	0.0(10)	−3.8(5)
χ^1	C(1p)-C(21)-C(2)-N(2)	−8.4(9)	−63.2(6)	−69.5(4)
χ^2	C(2p)-C(1p)-C(21)-C(2)	−26.4(9)	94.1(6)	107.9(4)
Out-of-plane parameters of the tertiary amides (°)				
χ_C		−3.2	−3.5	−2.8
χ_N		−7.9	3.6	0.1
τ		170.7	179.9	177.6

the N2H ...O2 = C hydrogen bond, leaving the tertiary amide free from strong interaction. In addition, the molecules in each of three crystals are joined by numerous C–H...O=C intermolecular contacts [26] involving both carbonyl groups (Table 3).

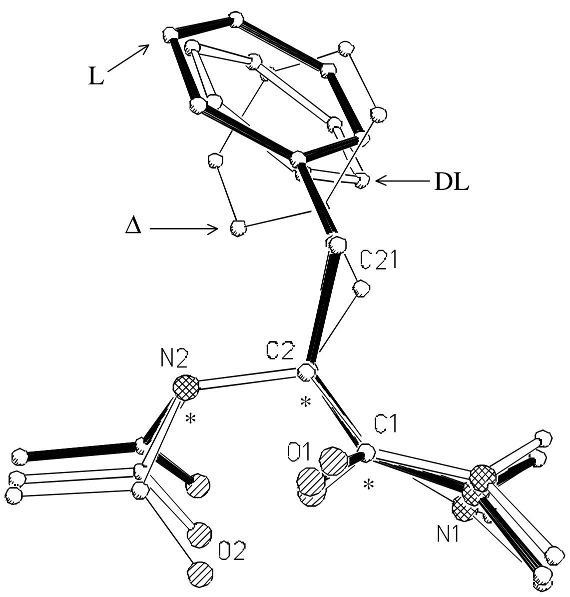

Figure 2 Three-point fit of three phenylalanine skeletons through the C1-C2-N2 fragment.

Theoretical Conformational Analysis

Figure 4A and 4B show the HF/3-21G energy maps *in vacuo*, in the ϕ, ψ torsion space for Ac-ΔAla-NMe$_2$ and Ac-(*Z*)-ΔPhe-NMe$_2$, respectively, with the HF/3-21G and DFT/B3LYP/6-31G** re-optimized minima. For clarity, the maps have been confined to the level of 7.0 kcal·mol^{-1}. This cut-off was assumed on the basis that 5.0 kcal·mol^{-1} is the limit between the allowed and disallowed regions of the Ramachandran map [27], plus 2.0 kcal·mol^{-1} as the maximum uncertainty in *ab initio* energy calculations at various levels [28], including our calculations (Table 4). Table 4 lists the selected conformational parameters of the above two molecules in the solid state and in all their energy-minimized conformers.

The conformational map of Ac-ΔAla-NMe$_2$ (Figure 4A) shows three minima and their mirror image with respect to inversion through the (0°, 0°) origin. The fully extended H-bonded C_5 conformer, $\phi, \psi = -179°$, 154°, constitutes the global, deep minimum. The second-lowest minimum at $\phi, \psi = -37°$, 124° is in region H of the Ramachandran diagram [27]. This region is of high-energy for common amino acids. The third minimum represents the other extended, but open structure D at $\phi, \psi = -178°$, 41°. The conformational map of Ac-(*Z*)-ΔPhe-NMe$_2$ (Figure 4B) has four minima plus their mirror image. The global minimum, $\phi, \psi = -37°$, 126°, is located in the area of the clearly

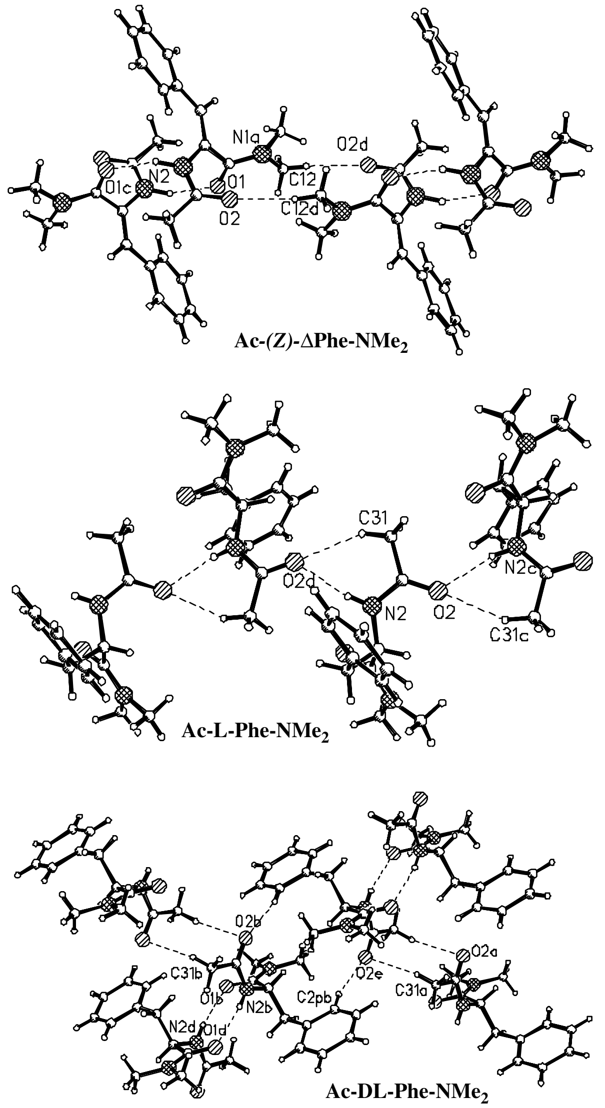

Figure 3 Association of molecules in the crystal structure. Hydrogen bonds are marked by dashed lines.

distinct topology, in region H of the Ramachandran diagram. The second-lowest minimum, $\phi, \psi = -130^\circ$, 148°, with a small magnitude of separation of only 1.1 kcal mol^{-1}, lies in the region of C_5 conformers (region E). The remaining minima are positioned as follows: in the upper-right quarter of the map, in region E* at $\phi, \psi = 126^\circ$, 157° and in region D at $\phi, \psi = -114^\circ$, 44°. In all conformers, the angle χ^2, is relatively small, does not exceed the value $|34^\circ|$, indicating a π-coupling tendency between the phenyl ring and the $C^\alpha{=}C^\beta$ bond. The tertiary amide of both molecules in all their conformers displays a significant non-planarity.

DISCUSSION

Folding Ac-(*Z*)-ΔPhe-NMe$_2$ in the solid state, $\phi, \psi = -49.5^\circ$, 132.6°, very much resembles the known solid state conformers of two other dehydro dimethylamides Ac-ΔAla-NMe$_2$ [1] and Ac-(*Z*)-ΔLeu-NMe$_2$ [29] as well as that of the only α, β-dehydro tertiary dipeptide [30] (Table 5). The respective angles ϕ, ψ, χ^1 are strikingly similar and do not depend on intermolecular contacts. All these structures show some non-planarity [31] of the *C*-terminal amide bond and are located in the high-energy region H/F of the Ramachandran map for common amino acids [27]. The free molecule calculations on Ac-ΔAla-NMe$_2$ and Ac-(*Z*)-ΔPhe-NMe$_2$, among the low-energy minima, found one close to its crystal conformer. This minimum with the identical backbone torsion angles for both molecules, $\phi, \psi = -37^\circ$, $125 \pm 1^\circ$ is positioned in region H of the Ramachandran plot, and has the strongly deformed *C*-terminal amide bond, in both cases identical (Table 4). The distortion results from the steric repulsion between the hydrogen atom in the β-position and that of the N'-methyl group. However, in the solid state, the out-of-plane parameters of the amide, especially χ_N defining the pyramidalization of the nitrogen atom are, as usual [14], reduced with respect to the theoretical values.

As is visible from the energy maps (Figure 4) there are essential differences in the overall conformational profile of the Ac-ΔAla-NMe$_2$ and Ac-(*Z*)-ΔPhe-NMe$_2$ molecules. For Ac-ΔAla-NMe$_2$, a significant area of the ϕ, ψ space is not available. This available space encompasses flat or quite flat conformers along and around the $\phi = \pm 180^\circ$, including those in the region of $\phi = 180^\circ \pm 25^\circ$ and $\psi = 0 \pm 50^\circ$, which is disallowed for common amino acids [27,32–35]. On the contrary, the Ac-(*Z*)-ΔPhe-NMe$_2$ molecule experiences a great conformational freedom and can accommodate a variety of structures, among others, those which are accessible only to D-amino acids [35], and those which the phenylalanine residue attains only exceptionally [34]. Despite these differences the localization of the energetic minima and the crystal structures of Ac-ΔAla-NMe$_2$ and Ac-ΔPne-NMe$_2$ are similar.

The above differences in overall conformational profiles and similarities in particular conformational minima between Ac-ΔAla-NMe$_2$ and Ac-ΔPhe-NMe$_2$ can be explained by the influence of the $C^\alpha{=}C^\beta$ double bond, which when introduced into an α-amino acid diamide aims at a π-cross-conjugated system [36,37]. This becomes the main

Table 3 Hydrogen-Bond Geometry and Contacts with C...O less than 3.60 Å[a] for Ac-(*Z*)-ΔPhe-NMe_2, Ac-L-Phe-NMe_2 and Ac-DL-Phe-NMe_2

	D···A (Å)	D-H (Å)	H···A (Å)	∠DHA (°)
Ac-(*Z*) – ΔPhe-NMe_2				
N2–H···O1$^{[2-x;1-y;1-z]}$	2.902(5)	1.02	1.92	159
C12–H···O1$^{[2-x;2-y;1-z]}$	3.397(7)	0.96	2.74	126
C31–H···O1$^{[2-x;1-y;1-z]}$	3.496(7)	0.96	2.68	143
C5p–H···O1$^{[x;y-1;z+1]}$	3.452(7)	0.93	2.69	140
C12–H···O2$^{[1-x;2-y;1-z]}$	3.455(7)	0.96	2.50	172
Ac-L-Phe-NMe_2				
N2–H···O2$^{[x+0.5;0.5-y;1-z]}$	2.948(8)	0.86	2.11	165
C11–H···O1$^{[1-x;0.5+y;0.5-z]}$	3.271(9)	0.96	2.81	111
C12–H···O1$^{[1-x;0.5+y;0.5-z]}$	3.347(10)	0.96	2.89	111
C31–H···O2$^{[x+0.5;0.5-y;1-z]}$	3.285(7)	0.96	2.41	152
C4p–H···O2$^{[0.5-x;1-y;0.5+z]}$	3.551(9)	0.93	2.64	168
Ac-DL-Phe-NMe_2				
N2–H···O1[-x; 1-y; 2-z]	2.892(4)	0.86	2.05	167
C11–H···O2[-x; 2-y; 2-z]	3.223(5)	0.96	2.81	107
C31–H···O2[1-x; 1-y; 2-z]	3.481(5)	0.96	2.54	165
C31–H···O1[-x; 1-y; 2-z]	3.573(5)	0.96	2.75	144
C21–H···O2[x-1; y; z]	3.484(4)	0.97	3.02	111
C6p–H···O2[-x; 2-y; 2-z]	3.327(5)	0.93	2.43	161

[a] This cut-off has been assumed on the basis of the average value of 3.6 Å for the C-H···O interactions in the crystal structures of dimethylformamide dimers [26].

Table 4 Selected Conformational Parameters of the Ac-ΔAla-NMe_2 and Ac-(*Z*)-ΔPhe-NMe_2 Molecules in the Solid State and in all their Energy-Minimized Conformers

Compound/Method	Conformer[a]	Energy (kcal·mol^{-1})	ϕ	ψ	χ^2	χ_C	χ_N	τ
Ac-ΔAla-NMe_2								
X-ray	H/F	—	−42.4	127.2	—	−5.5	−11.0	171.6
B3LYP/6 – 31**G	E	0.0	179.0	153.9	—	−2.1	−16.7	164.0
	H	4.2	−37.3	123.8	—	−6.6	−26.2	168.0
	D	4.8	−178.3	40.7	—	3.9	31.9	−160.1
HF/3-21G	E	0.0	−179.4	157.2	—	−1.5	−15.5	160.8
	D	3.4	−178.5	30.4	—	3.5	36.1	−150.7
	F	5.7	−44.1	130.1	—	−5.1	−26.8	162.4
Ac-(*Z*) – ΔPhe-NMe_2								
X-ray	F	—	−49.5	132.6	−26.4	−3.2	−7.9	170.7
B3LYP/6-31**G	H	0.0	−37.1	126.4	−29.7	−6.4	−26.2	167.6
	E	1.1	−130.4	148.0	16.5	−2.5	−17.8	163.8
	E*	3.1	126.4	157.0	−19.6	−1.3	−22.3	160.3
	D	4.8	−114.7	44.4	−33.7	3.4	20.6	−164.1
HF/3-21G	H/F	0.0	−43.3	132.2	−43.1	−4.9	−27.9	161.1
	D	0.6	−111.2	34.1	−56.3	2.0	16.4	−161.3
	H*	1.4	39.8	43.3	50.8	−3.5	3.3	−165.3
	E	2.7	−129.1	149.4	31.7	−2.3	−18.1	160.2
	E*	5.6	120.0	158.0	−28.0	−0.9	−22.5	155.7

[a] The conformers are labelled according to the name of the Ramachandran map regions [27].

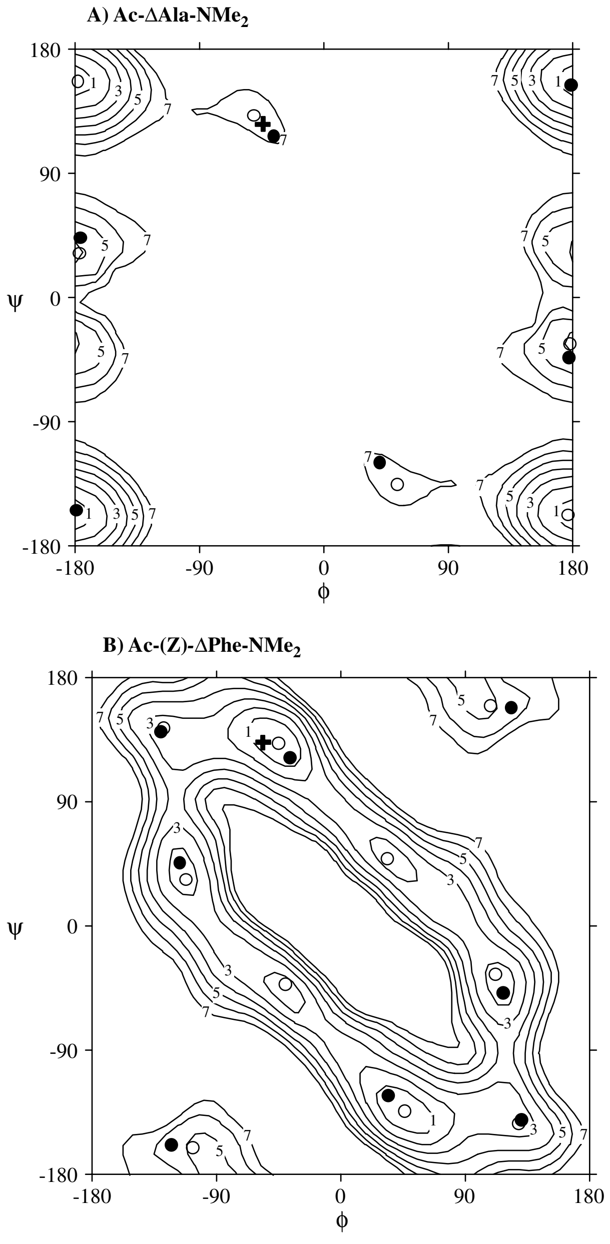

Figure 4 The energy maps of A) Ac-ΔAla-NMe$_2$ (15° spacing) and B) Ac-(Z)-ΔPhe-NMe$_2$ (30° spacing) in the ϕ, ψ space *in vacuo* at the *ab initio* HF/3-21G level of theory. The isopotential lines are spaced by 1 kcal·mol^{-1}. + Crystal structures, ○ HF/3-21G minima, ● DFT/B3LYP/6-31G** minima.

driving force for the conformational behaviour of the α,β-dehydroamino acid diamides and is most clearly seen for dehydroalanine, which deprived of any β-substituent is capable of realising the π-cross-conjugation most fully. For dehydroalanine dimethyldiamide, the planar E conformer is the global minimum. This conformer has the internal C_5 hydrogen bond and significantly π-conjugated system [1]. Therefore it constitutes the deep minimum and the consecutive minima H and D, in which some π-conjugation is expected [36,37], are much richer in energy. The molecule has a determined tendency to reside in this most π-conjugated state and a significant area of conformational space is not accessible for it. Within the dehydrophenylalanine dimethyldiamide, the phenyl ring provides a steric constraint on the backbone torsion angle ϕ and repulsive electrostatic interaction at the carbonyl oxygen of the acetyl group (Figure 5), which prevents the molecule from assuming this fully extended conformation at its *N*-terminus, as adopted by the dehydroalanine counterpart. This along with another constraint, provided by the dimethylamide group on the backbone torsion angle ψ, causes the structure E of Ac-(*Z*)-ΔPhe-NMe$_2$ to be strongly warped, weakly H-bonded and with a small extent of π-conjugation [37]. As a result, the other π-conjugated conformer is that with the lowest energy. This is conformer H, in which the amide hydrogen is appropriately oriented and at the right distance to the nearest aromatic C atom (Figure 5), so a weak attractive interaction NH$\cdots\pi$ between it and the π-face of the phenyl ring can occur [38,39]. Various weakly π-conjugated and energetically similar states are possible for this free molecule and it can occupy a large part of the conformational space.

The solvation by H-bond forming solvents [40,41] or the packing in crystal [41] stabilizes preferentially, sometimes by more than 3 kcal·mol^{-1}, the open structures that are energetically unfavourable in the gas phase. This is expected in view of the greater potential for intermolecular hydrogen bonding possessed by these structures. Both Ac-ΔAla-NMe$_2$ and Ac-(*Z*)-ΔPhe-NMe$_2$ are proton-deficient, each molecule contains only one N–H-bond. Of the open conformers of these compounds, conformer H only has this H-bond donor most exposed on the outside of the molecule. Hence this conformation forms the crystal phase.

Passing to the structural properties of the sample saturated analogues we find them to be in line with other compounds in the series of L/DL dimethylamides. The solid state conformer of Ac-L-Phe-NMe$_2$, $\phi, \psi = -99.3°, 148.5°$, differs from that of Ac-(*Z*)-ΔPhe-NMe$_2$. It also differs from those of other known acetyl-L-amino acid dimethylamides (Table 5 in [1]). Its angles ϕ, ψ are halfway between the angles of Ac-L-Ala-NMe$_2$ and Ac-L-Met-NMe$_2$, and

Table 5 Selected Solid State Conformational Parameters and Molecular Association Patterns for Ac-ΔXaa-NR_2

Compound	ϕ	ψ	χ^1	χ^2	χ_C	χ_N	τ	Association pattern	Ref.
Ac-ΔAla-NMe_2	−42.4	127.2	0.0	—	−5.5	−11.0	171.6	Chain: *N*- to *C*-terminus	[1]
Ac-(Z)-ΔLeu-NMe_2	−42.2	127.3	−3.2	109.4	−4.9	−14.7	171.3	Centrosymmetric dimer	[29]
Ac-(Z)-ΔPhe-NMe_2	−49.5	132.6	−8.4	−26.4	−3.2	−7.9	170.7	Centrosymmetric dimer	this work
Ac-(Z)-ΔPhe-Pro 1/2 H_2O	−56.8	148.7	−7.0	−39.8	−1.9	−6.8	174.6	Dimer around 2-fold axis	[30]

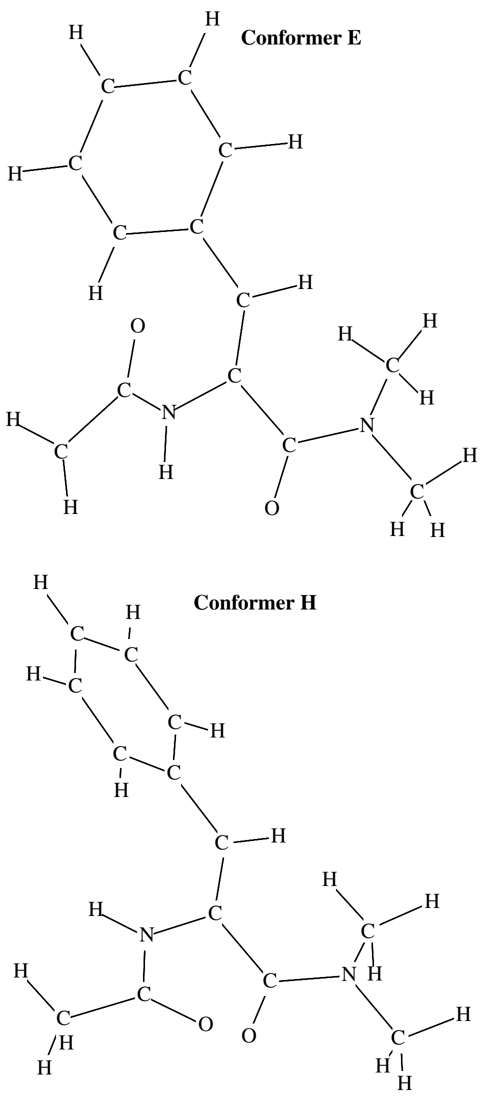

Figure 5 The E and H conformers of the Ac-(Z)-ΔPhe-NMe_2 molecule obtained with the DFT/B3LYP/6-31**G method.

far away from the angles of Ac-L-Val-NMe_2. The conformation of the molecule of L-configuration in the crystal of Ac-DL-Ala-NMe_2 or Ac-DL-Phe-NMe_2 is very similar to that in the crystal of Ac-L-Ala-NMe_2 or Ac-L-Phe-NMe_2, respectively, whereas in the pair of analogous L/DL-Val compounds, there is no likeness. So, in contrast to the conservative conformation of the unsaturated amides Ac-ΔXaa-NMe_2, which is independent of packing forces, the molecular conformations of the saturated Ac-L/DL-Xaa-NMe_2 are various, no regular resemblance can be found, and additionally they can be strongly affected by the packing mode.

Ac-(*Z*)-ΔPhe-NMe_2 and Ac-DL-Phe-NMe_2 associate in the form of a centrosymmetric dimer with hydrogen bonding, which is characteristic of Ac-(*Z*)-ΔLeu-NMe_2 and typical of other Ac-DL-Xaa-NMe_2, where Xaa = Leu, Tle, Val (Table 5 in [1]). Ac-L-Phe-NMe_2 associates in infinite chains, the *N*-terminus to the *N*-terminus by the hydrogen bond, which is typical of Ac-L-Xaa-NMe_2 molecules, where X = Ala, Met, Val. In contrast to the lack of one conformational pattern, we see the constant associative pattern in the analysed saturated compounds. Only the ΔAla and DL-Ala dimethylamides, with the shortest side chain, atypically form infinite catemers [1].

CONCLUSION

The studied diamides Ac-ΔXaa-NMe_2 combine the double bond in positions α, β and the *C*-terminal tertiary amide within one molecule. As the representative probe with ΔXaa = ΔAla [1], (*Z*)-ΔLeu [29] and (*Z*)-ΔPhe (this work) shows, in the solid state they adopt the conservative conformation with $\phi, \psi \sim -45^\circ$, $\sim 130^\circ$ and with a non-planar tertiary amide bond, whatever the packing forces are. This conformation is located on the Ramachandran map in region H/F, which is of high-energy for common amino acids, but not so readily accessible to them. The *ab initio* free molecule calculations on Ac-ΔAla-NMe_2 and Ac-(*Z*)-ΔPhe-NMe_2 reveal, that in spite of the dissimilar overall conformational profiles of these molecules, this structure is one of their low-energy conformers and for Ac-(*Z*)-ΔPhe-NMe_2 it constitutes the global minimum. So, the theoretical results corroborate the experimental results proving that this structure is robust enough to avoid conformational distortion due to packing forces. In contrast to Ac-ΔXaa-NMe_2, the saturated Ac-L/DL-Xaa-NMe_2 shows the constancy of the associative patterns but does not prefer any molecular structure in the solid state.

Acknowledgements

The authors gratefully acknowledge the University of Opole for grant number 9/ICh/2002-W and the Academic Computer Center CYFRONET AGH of Kraków for grant number KBN/SGI2800/UOpolski/011/2001.

REFERENCES

1. Rzeszotarska B, Siodłak D, Broda MA, Dybała I, Kozioł AE. Conformational investigation of α,β-dehydropeptides. X. Molecular and crystal structures of Ac-ΔAla-NMe_2 as compared to those of Ac-L-Ala-NMe_2, Ac-DL-Ala-NMe_2 and other dimethylamides. *J. Peptide Res.* 2002; **59**: 79–89 and references therein.
2. Siodłak D, Broda MA, Rzeszotarska B, Kozioł AE, Dybała I. Conformational properties of *N′N′*-dimethylamides of *N*-acetyldehydroalanine and *N*-acetyldehydrophenylalanine. *Acta Biochim. Polon.* 2001; **48**: 1179–1183.
3. Hruby VJ, Li G, Haskell-Luevano C, Shenderovich M. Design of peptides, proteins, and peptidomimetics in chi space. *Biopolymers (Peptide Sci.)* 1997; **43**: 219–266.
4. Hruby VJ, Balse PM. Conformational and topographical considerations in designing agonist peptidomimetics from peptide leads. *Curr. Med. Chem.* 2000; **7**: 945–970.
5. Hruby VJ. Design in topographical space of peptide and peptidomimetic ligands that affect behavior. A chemist's glimpse at the mind–body problem. *Acc. Chem. Res.* 2001; **34**: 389–397.
6. Bovy PR, O'Neal JM, Olins GM, Patton DR, McMohan EG, Palomo M, Koepke JP, Salles KS, Trapani AJ, Smits GJ, McGraw DE, Hutton WC. Structure–activity relationships for the carboxy-terminus truncated analogues of angiotensin II, a new class of angiotensin II antagonists. *J. Med. Chem.* 1990; **33**: 1477–1482.
7. Vitoux B, Aubry A, Cung MT, Marraud M. *N*-Methyl peptides. VII. Conformational perturbations induced by *N*-methylation of model dipeptides. *Int. J. Peptide Protein Res.* 1986; **27**: 617–632.
8. Aubry A, Marraud M. Pseudopeptides and β-folding: x-ray structures compared with structures in solution. *Biopolymers* 1989; **28**: 109–122.
9. Barton PS, Cinradi RA, Hilgers AR, Ho NFH, Maggiora LL. The relationship between peptide structure and transport across epithelial cell monolayers. *J. Controlled Release* 1992; **19**: 87–98.
10. Cinradi RA, Hilgers AR, Ho NFH, Barton PS. The influence peptide structure on transport across Caco-2 cells. II. Peptide bond modification which results in improved permeability. *Pharm. Res.* 1992; **9**: 435–439.
11. Cody WL, He JX, Reily MD, Haleen SJ, Walker DM, Reyner EL, Stewart BH, Doherty AM. Design of a potent combined pseudopeptide endothelin-A/endothelin-B receptor antagonist, Ac-DBhg^{16}-Leu-Asp-lle-[NMe]lle-Trp^{21} (PD 156252): examination of its pharmacokinetic and spectral properties. *J. Med. Chem.* 1997; **40**: 2228–2240.
12. Marraud M, Dupont V, Grand V, Zerkout S, Lecoq A, Boussard G, Vidal J, Collet A, Aubry A. Modification of the amide bond and conformational constraints in pseudopeptide analogues. *Biopolymers* 1993; **33**: 1135–1138.
13. Gao J, Sudoh J, Aubé J, Borchard RT. Transport characteristics of peptides and peptidomimetics: I. *N*-methylated peptides as substrates for the oligopeptide transporter and P-glycoprotein in the intestinal mucosa. *J. Peptide Res.* 2001; **57**: 316–329.
14. Boks GJ. *Structure and Conformational Behaviour of Peptoid Peptidomimetics*, 1997; http://pablo.ubu.ruu.n./~proefsch/01741627/boks.html.
15. Greenstein JP, Winitz M. *Chemistry of the Amino Acids, Vol. 3.* Wiley: New York, 1961; 1831.
16. Herbst RM, Shemin D. *α-Acetaminocinnamic acid. Org. Synth. Coll. Vol. 2*, Wiley: New York, 1943; 1–3; Wong HNC, Xu ZL, Chang HM, Lee CM. A modified synthesis of (±)-β-aryllactic acids. *Synthesis* 1992; 793–797.
17. Saitō I, Kikugawa Y, Yamada S. Chemistry of diborane and sodium borohydride. VII. Reduction of α-amino acid amides with sodium borohydride. *Chem. Pharm. Bull.* 1970; **18**: 1731–1736.
18. Sheldrick GM. *SHELXS-97: Program for Structure Solution.* University of Göttingen: Göttingen, 1997.
19. Sheldrick GM. *SHELXL-97: Program for the Refinement of Crystal Structures from Diffraction Data.* University of Göttingen: Göttingen, 1997.
20. Becke AD Density-functional thermochemistry III. The role of exact exchange. *J. Chem. Phys.* 1993; **98**: 5648–5652.

21. Frisch MJ, Trucks GW, Schlegel HB, Scuseria GE, Robb MA, Cheeseman JR, Zakrzewski VG, Montgomery JA, Stratmann RE, Burant JC, Dapprich S, Millam JM, Daniels AD, Kudin KN, Strain MC, Farkas O, Tomasi J, Barone V, Cossi M, Camm R, Mennucci B, Pomelli C, Adamo C, Clifford S, Ochterski J, Petersson GA, Ayala PY, Cui Q, Morokuma K, Malick DK, Rabuck AD, Raghavachari K, Foresman JB, Cioslowski J, Ortiz JV, Stefanov BB, Liu G, Liashenko A, Piskorz P, Komaromi I, Gomperts R, Martin RL, Fox DJ, Keith T, Al-Laham MA, Peng CY, Nanayakkara A, Gonzalez C, Challacombe M, Gill PMW, Johnson B, Chen W, Wong MW, Andres JL, Head-Gordon M, Replogle ES, Pople JA. *Gaussian 98, Revision A.3*, Gaussian, Inc.: Pittsburgh, 1998.
22. Benedetti E. Peptide X-ray crystallographic determination. In *Chemistry and Biochemistry of Amino Acids, Peptides and Proteins. Vol. 6*, Weinstein B (ed.). Marcel Dekker: New York, 1982; 105–184.
23. Jain R, Chauhan VS. Conformational characteristics of peptides containing α,β-dehydroamino acids residues. *Biopolymers (Peptide Sci.)* 1996; **40**: 105–119.
24. Winkler FK, Dunitz JD. The non-planar amide group. *J. Mol. Biol.* 1971; **59**: 169–182.
25. Dunitz JD, Winkler FK. Amide group deformation in medium-ring lactams. *Acta Cryst.* 1975; ***B31***: 251–263.
26. Vargas R, Garza J, Dixon DA, Hay BP. How strong is the C^{α}–H... O=C hydrogen bond? *J. Am. Chem. Soc.* 2000; **122**: 4750–4755.
27. Zimmerman SS, Pottle MS, Némethy G, Scheraga HA. Conformational analysis of the 20 naturally occurring amino acid residues using ECEPP. *Macromolecules* 1977; **10**: 1–9.
28. Frey RF, Coffin J, Newton SQ, Ramek M, Cheng VKW, Momany FA. Schäfer L. Importance of correlation-gradient geometry optimization for molecular conformational analyses. *J. Am. Chem. Soc.* 1992; **114**: 5369–5378.
29. El-Masdouri L, Aubry A, Boussard G, Marraud M. Structural variations in the crystal structures of two homologous DL-Leu and ΔLeu containing peptides. *Int. J. Peptide Protein Res.* 1992; **40**: 482–486; Erratum *Int. J. Peptide Protein Res.* 1993; **41**: 612.
30. Ajo D, Busetti V, Granozzi G. Conformational flexibility of dehydroalanine derivatives. Crystal and molecular structure of -*N*-acetyldehydrophenylalanyl-L-proline. *Tetrahedron* 1982; **38**: 3329–3334.
31. Ashida T, Tsunogae Y, Tanaka I, Yamane T. Peptide chain structure parameters, bond angles and conformational angles from the Cambridge Structural Database. *Acta Cryst.* 1987; **B43**: 212–218.
32. Roterman IK, Lambert MH, Gibson KD, Scheraga HA. A comparison of the CHARMM, AMBER and ECEPP potentials for peptides. II. ϕ-ψ Maps for *N*-acetyl alanine *N*-methyl amide: comparisons, contrasts and simple experimental tests. *J. Biomol. Struct. Dynam.* 1989; **7**: 421–453.
33. Gould IR, Cornell WD, Hillier IH. A quantum mechanical investigation of the conformational energetics of the alanine and glycine dipeptides in the gas phase and in aqueous solution. *J. Am. Chem. Soc.* 1994; **116**: 9250–9256.
34. Jákli J, Perczel A, Farkas O, Hollosi M, Csizmadia TG. Peptide models XXII. A conformational model for aromatic amino acid residues in proteins. A comprehensive analysis of all the RHF/6-31GH* conformers of For-L-Phe-NH_2. *J. Mol. Struct. (Theochem)* 1998; **455**: 303–314.
35. Venkatraman J, Shankaramma SC, Balaram P. Design of folded peptides. *Chem. Rev.* 2001; **101**: 3131–3152.
36. Thormann M, Hofmann H-J. Conformational properties of peptides containing dehydro amino acids. *J. Mol. Struct. (Theochem)* 1998; **431**: 79–96.
37. Broda MA, Rzeszotarska B. α,β-Dehydropeptides at the residue level: conformation and amidic resonance. In *Peptides 1998. Proc. 25th Eur. Pept. Symp., 1998 Budapest, Hungary*, Bajusz S, Hudecz F (eds). Akadémiai Kiadó: Budapest, 1999; 452–453.
38. Molone JF, Murray CM, Charlton MH, Docherty R, Lavery AJ. X — H...π (phenyl) interactions. Theoretical and crystallographic observations. *J. Chem. Soc. Faraday Trans.* 1997; **93**: 3429–3436.
39. Tsuzuki S, Honda K, Uchimaru T, Mikami M, Tanabe K. Origin of the attraction and directionality of the NH/π interaction: comparison with OH/π and CH/π interactions. *J. Am. Chem. Soc.* 2000; **122**: 11 450–11 458.
40. Buesnel R, Hillier IH, Masters AJ. A molecular dynamics study of the conformation of alanine dipeptide in aqueous solution using a quantum mechanical potential. *Mol. Phys.* 1997; **90**: 787–792.
41. Bohr HG, Frimand K, Jalkanen KJ, Nieminen RM, Suhai S. Neural-network analysis of the vibrational spectra of *N*-acetyl-L-alanyl *N*-methyl amide conformational states. *Phys. Rev. E* 2001; **64**: 021905 1–13.

